Springer

KSME

Journal of Mechanical Science and Technology 29 (11) (2015) 4891~4900
www.springerlink.com/content/1738-494x(Print)/1976-3824(Online)
DOI 10.1007/s12206-015-1037-6

Hopping system control with an approximated dynamics model and upper-body motion †

Hyangjun Lee and Junho Oh*

Department of Mechanical Engineering, Korea Advanced Institute of Science and Technology, Daejeon, 305-701, Korea

(Manuscript Received June 19, 2014; Revised March 31, 2015; Accepted June 13, 2015)

Abstract

A hopping system is highly non-linear due to the nature of its dynamics, which has alternating phases in a cycle, flight and stance phases and related transitions. Every control method that stabilizes the hopping system satisfies the Poincaré stability condition. At the Poincaré section, a hopping system cycle is considered as discrete sectional data set. By controlling the sectional data in a discrete control form, we can generate a stable hopping cycle. We utilize phase-mapping matrices to build a Poincaré return map by approximating the dynamics of the hopping system with SLIP model. We can generate various Poincaré stable gait patterns with the approximated discrete control form which uses upper-body motions as inputs.

Keywords: Dynamics approximation; Hopping cycle; Legged robot; Poincaré stability; SLIP (Spring-loaded inverted pendulum)

1. Introduction

A legged locomotion system is a basic form of legged living creatures, so researches on legged locomotion have been done to understand its nature. In mechanical engineering, this type of system is defined as a hybrid system [1] that has continuous phases and discrete transitions. Since Raibert's study [2, 3], one-legged hoppers with a Spring loaded inverted pendulum (SLIP) model have been studied widely in experiments [4, 5], theories [6-8] and biomechanics [9]. Blickhan and Full showed that legged-animal locomotion could be modelled as a monopod, which well describes animal motion [9]. The SLIP model hopper is simple and a good model template for legged locomotion for many studies [4, 5, 10-13]. The controller of the legged locomotion, however, is hard to derive, as the model is non-linear hybrid dynamics. Raibert introduced a heuristic foot-placement controller, which was a huge success [2]. Ahmadi and Buehler developed a control method using foot-placement [5]. Their controller matches the passive dynamics and motion of the foot, getting the neutral point and conserving energy. François and Samson derived a controller different from Raibert's [14]. They developed a control method using Poincaré map near the fixed point and feedback control to get asymptotically stable gaits. Morris and Grizzle proposed Hybrid Zero Dynamics and Poincaré map based control method [15]. These controllers utilize the Poincaré map created by approximation and constraints [5, 14-19]. The approximation methods of stance phase motion have been developed by many researchers, such as Schwind, Geyer and Saranli [20-22]. They approximate the stance phase motion into mapping matrices. We adopt SLIP model with upper-body and use the upper-body motion to generate gait patterns. The modelled hopping system has three distinctive inputs in a cycle: leg thrust at stance phase and joint rotations at both continuous phases. These are time sequential inputs in a hopping cycle and the hopper is defined as a multi-input single-output (MISO) system with these inputs. From former studies, the hopping system is controlled with constraints of model, dynamics and gait patterns [10, 15, 23-25]. We propose an active use of feedback by upper-body motion to generate gait patterns. We utilize the upper-body motion trajectory as inputs and approximate the continuous phase iteratively, constraining the leg thrust. Designing a hopping system controller is solving a hybrid non-linear dynamics problem with periodic phases. We simplify the hopping system to a simple discrete control form and solve it. We present mapping matrices of hopping system with upper-body motion, which are transverse linearization of the continuous phases and discrete transitions, to redefine the hopping problem into a discrete control form. We can stabilize the system through feedback of Poincaré return map created by the mapping [24]. And we can generate several gait patterns through different upper-body motion combinations of both flight and stance phases. We chose a SLIP model here of a one-legged hopper. Its mathematical model and the hopping cycle are reviewed in Sec. 2. In Sec. 3,

*Corresponding author. Tel.: +82 42 350 3263 , Fax.: +82 42 350 8900
E-mail address: jhoh@kaist.ac.kr
† Recommended by Associate Editor Yang Shi

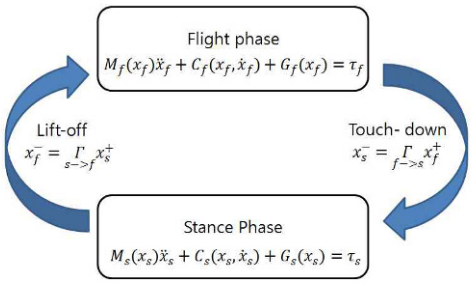

Fig. 1. Hopping cycle.

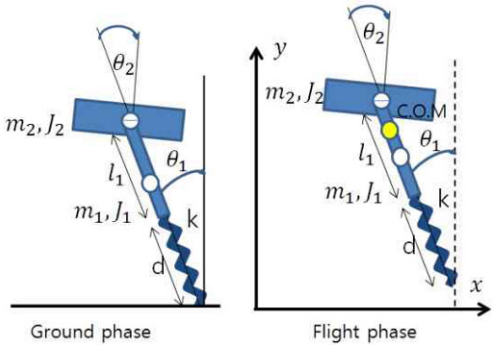

Fig. 2. SLIP model of hopping system.

we deal with constraints and approximation of the Poincaré map. The gait pattern generation derived from motion planning and stabilization by feedback of the Poincaré map is shown in Sec. 4. Simulation results and discussions of them are presented in Sec. 5. The conclusion is given in Sec. 6.

2. Mathematical model

$$\begin{cases} M_s(x_s)\ddot{x}_s + C_s(x_s,\dot{x}_s) + G_s(x_s) = \tau_s \\ x_f^- = \Gamma_{s->f} x_s^+ \\ M_f(x_f)\ddot{x}_f + C_f(x_f,\dot{x}_f) + G_f(x_f) = \tau_f \\ x_s^- = \Gamma_{f->s} x_f^+ \end{cases} . \quad (1)$$

The hopping system is a simple and well known platform for legged locomotion [2-4, 6-9, 14, 17, 20, 21, 26, 27]. The distinctive characteristics of legged locomotion, compared to a wheel based system, is discontinuity in a cycle. A hopping cycle consists of two continuous phases, flight phase and stance phase, and two discrete transitions, touch-down transition and lift-off transition, in Fig. 1. A dynamic system with these features is defined as a hybrid system [1]. The solution for this type of hybrid system is hard to achieve. Researchers have dealt with the problem by modelling and putting constraints on it. We adopt a Spring-loaded inverted pendulum (SLIP) with upper-body model, spring loaded double-inverted pendulum, for the hopper. In Fig. 2, a schematic of the model is shown, consisting of two masses and inertias of upper-body and lower-body, one actuated joint between, and a spring-loaded leg at the foot. The contact point on the ground is assumed to be in non-slip condition. The SLIP model has a spring-loaded leg, and the length of the leg is limited. In this paper, the hopping system is analyzed on the sagittal plane.

2.1 Governing equations of modelled system

The mathematical modelling of a hopping system is derived for each continuous phase and discrete transition. The governing equations of continuous phases are derived by Lagrangian method, and the transitions are assumed to occur instantly. The hopping system is modelled in simple SLIP with upper-body.

2.1.1 Stance phase dynamics

Stance phase dynamics is that of a spring-loaded double-inverted pendulum. It is presented on polar coordinate, clock-wise positive. The stance-phase states are $x_s = [\theta_1, \theta_2, d]$, respectively, indicating the global angle for the leg, the joint angle of the upper-body, and the spring length. The system consists of point mass and inertia at its upper-body and lower-body.

$$M_s(x_s)\ddot{x}_s + C_s(x_s,\dot{x}_s) + G_s(x_s) = \tau_s , \quad (2)$$
$$\tau_s = \begin{bmatrix} \tau_{1s} & \tau_{2s} & f_s \end{bmatrix}.$$

Here, the torques and force are inputs, which represent contact point torque, joint torque and thrust of leg, respectively. The motion of stance phase follows the governing equation, Eq. (2); equation details are in the appendix. With appropriate constraints, we can approximate the motion of stance phase [20, 22, 28, 29].

2.1.2 Lift-off transition

Lift-off is the time section that the hopper is detached from the ground. The hopper dynamics changes from the stance phase to the flight phase. The system dynamic changes from the double-inverted pendulum to the ballistic system. Lift-off transition occurs instantly and the physical properties are continuous. At lift-off transition, the physical properties of the hopping system are continuous, such as velocities and positions. The system dynamics changes from the stance phase to flight phase. The local state of the stance phase is $x_s = [\theta_1, \theta_2, d]$ and the local state of flight phase is $x_f = [\theta_1, \theta_2, x, y]$. The lift-off transition is expressed in a matrix, $\Gamma_{s->f} = f_3(x_s^+)$ Eq. (3); change the stance phase boundary value, before lift-off x_s^+, into flight phase boundary value, after lift-off x_f^-, equation details are in Appendix.

$$x_f^- = \Gamma_{s->f} x_s^+ \quad (3)$$
$$x_s^+ = [\theta_{1lo}^-, \dot{\theta}_{1lo}^-, \theta_{2lo}^-, \dot{\theta}_{2lo}^-, d_{lo}, \dot{d}_{lo}] \quad \text{to}$$
$$x_f^- = [\theta_{1lo}^+, \dot{\theta}_{1lo}^+, \theta_{2lo}^+, \dot{\theta}_{2lo}^+, x_{lo}, \dot{x}_{lo}, y_{lo}, \dot{y}_{lo}] .$$

The boundary conditions have constraints. The joint velocities $\dot{\theta}_{2lo}^-$ and $\dot{\theta}_{2lo}^+$ are zero by designed trajectory of joint and

the Cartesian positions x_{lo}, y_{lo} are assumed to be in local coordinate that has a origin at the tip of the hopper.

2.1.3 Flight phase dynamics

Flight phase dynamics is a ballistic motion as a whole with a joint rotation. The flight-phase states, $x_f = [\theta_1, \theta_2, x, y]$, are explained in the order, the global angle of the lower body, the joint angle of the upper body related to the lower body(the angles are clock-wise positive), and the position of COM (Center of mass) in Cartesian coordinate.

$$M_f(x_f)\ddot{x}_f + C_f(x_f, \dot{x}_f) + G_f(x_f) = \tau_f, \quad (4)$$
$$\tau_f = \begin{bmatrix} \tau_{1f} & \tau_{2f} & f_x & f_y \end{bmatrix}.$$

The inputs of flight phase are the torques and forces, which represent external global angular torque, joint torque, and external force in Cartesian coordinate, respectively. The motion of flight phase follows the governing equation, Eq. (4); equation details are in appendix. With appropriate constraints, we can approximate the motion of flight phase.

2.1.4 Touch-down transition

Touch-down is the moment when the hopper contacts the ground. Touch-down transition is defined as a perfect plastic collision. And the impact occurs instantly and is governed by angular momentum conservation. The hopper dynamics changes from the flight phase to the stance phase. The system dynamic changes from the ballistic system to the double-inverted pendulum. At touch-down transition, the physical properties of the hopping system change, such as velocities and angular velocities, following the angular momentum conservation rule. The system dynamics changes from the flight phase to stance phase, instantly. The local state of the flight phase is $x_f = [\theta_1, \theta_2, x, y]$ and the local state of stance phase is $x_s = [\theta_1, \theta_2, d]$. The touch-down transition is expressed in a matrix, $\Gamma_{f->s} = f_6\left(x_f^+\right)$ Eq. (5); change the flight phase boundary value, before touch-down x_f^+, into stance phase boundary value, after touch-down x_s^-.

$$x_s^- = \Gamma_{f->s}\, x_f^+ \quad (5)$$
$$x_f^+ = [\theta_{1td}^-, \dot{\theta}_{1td}^-, \theta_{2td}^-, \dot{\theta}_{2td}^-, x_{td}, \dot{x}_{td}, y_{td}, \dot{y}_{td}],$$
$$x_s^- = [\theta_{1td}^+, \dot{\theta}_{1td}^+, \theta_{2td}^+, \dot{\theta}_{2td}^+, d_{td}, \dot{d}_{td}].$$

The boundary conditions have constraints. The joint velocities $\dot{\theta}_{2lo}^-$ and $\dot{\theta}_{2lo}^+$ are zero by designed trajectory of joint and the Cartesian positions x_{td}, y_{td} are on the coordinate that has a origin at the tip of the hopper. The ground is considered flat; equation details are in the appendix. If the ground is uneven, the touch-down transition changes according to inclination.

2.2 Poincaré map

The hybrid dynamics of a hopping system is stable when the Poincaré section of the system is non-diverging [14-17, 19, 30-32]. When we select after-lift-off state x_f^- as Poincaré section, the Poincaré return map has a matrix form that relates the selected time point of continuous cycle states to sequential next step states.

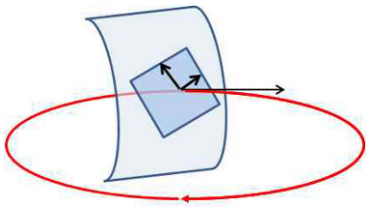

Fig. 3. Visualization of Poincare' surface.

$$\begin{cases} x_s^+ = f_s(x_s^-, U_s) \\ x_f^- = \Gamma_{s->f}\, x_s^+ \\ x_f^+ = f_f(x_f^-, U_f) \\ x_s^- = \Gamma_{f->s}\, x_f^+ \end{cases} \quad x_f^- = \Gamma_{s->f} f_s(\Gamma_{f->s} f_f(x_f^-, U_f), U_s). \quad (6)$$

The Poincaré map is approximated with constraints in Sec. 3 and it is simplified into a discrete control with upper-body motions as inputs.

3. Mapping by approximation and constraints

We approximate the whole cycle to linear matrices to generate a linear Poincaré map. The mathematical model is non-integrable without constraints. We constrain the inputs of the upper-body and vertical cycle of the system to map the phases in linear matrices.

3.1 Controller constraints

The constraints here are inputs of the upper-body which have designed shape and duration. And vertical motion is regulated to be considered as constant at transitions [5, 13].

3.1.1 The upper-body input

The upper-body motion is designed as a sinusoidal function during the continuous phases and as a stop at transitions. The upper-body motion is designed as below.

$$\begin{cases} \theta_{2s}(t) = C_s\left(1 - \cos\left(\omega_{2s} t\right)\right) + D_s & : stance\ phase \\ \theta_{2lo}^+ = \theta_{2lo}^- & : lift-off \\ \theta_{2f}(t) = C_f\left(1 - \cos\left(\omega_{2f} t\right)\right) + D_f & : flight\ phase \\ \theta_{2td}^+ = \theta_{2td}^- & : touch-down \end{cases} \quad (7)$$
$$\omega_{2s} = \frac{\pi}{t_s}, \quad D_s = \theta_{2td}^+, \quad C_s = \frac{\Delta\theta_{2s}}{2},$$
$$\omega_{2f} = \frac{\pi}{t_f}, \quad D_f = \theta_{2lo}^+, \quad C_f = \frac{\Delta\theta_{2f}}{2}.$$

3.1.2 The vertical cycle

Vertical motion of a hopping system is restricted in the total energy regulation [5]. The total energy is a sum of kinetic and potential energy of the system.

$$E_{design} = (m_1 + m_2) g \sin(\theta_1) + \frac{1}{2}(m_1 + m_2)(\dot{x}^2 + \dot{y}^2) + \frac{1}{2}(J_1 + J_2)\dot{\theta}_1^2$$
$$E_{design} - E_{estimate} = E_{loss} . \quad (8)$$

We compensate the energy loss during stance phase.

3.2 Mapping through Approximation

We approximate the whole cycle to linear matrices to generate a linear Poincaré map. We map the dynamics of the phases in transverse linear matrices to match the states of boundaries. We approximate the dynamics that includes the constrained conditions.

3.2.1 Stance phase dynamics mapping

We approximate the dynamic motion of stance phase to linear matrix by mapping after-touch-down states, $x_s^- = [\theta_{1td}^+, \dot{\theta}_{1td}^+, \theta_{2td}^+, \dot{d}_{td}]$ to before-lift-off states, $x_s^+ = [\theta_{1lo}^-, \dot{\theta}_{1lo}^-, \theta_{2lo}^-, \dot{d}_{lo}]$. We make non-linear parts of dynamics of the system integrable by using Taylor series of non-linear parts and gravity compensation [21, 22]. When the upper-body motion is given in constraints, the stance phase dynamics is approximated in a mapping matrix form below.

$$x_s^+ = A_s x_s^- + B_s \Delta\theta_{2s}$$
$$x_s^- = [\theta_{1td}^+, \dot{\theta}_{1td}^+, \theta_{2td}^+, \dot{d}_{td}], \quad x_s^+ = [\theta_{1lo}^-, \dot{\theta}_{1lo}^-, \theta_{2lo}^-, \dot{d}_{lo}]$$
$$\begin{cases} \theta_{1lo}^- = \dot{\theta}_{1m}(t_s) + \dot{\theta}_{1grav}(t_s) \\ \dot{\theta}_{1lo}^- = \theta_{1m}(t_s) + \theta_{1grav}(t_s) \\ \theta_{2lo}^- = \theta_{2s}(t_s) = \theta_{2td}^+ + \Delta\theta_{2s} \\ \dot{d}_{lo} = -\dot{d}_{td} \end{cases} \quad (9)$$

$$\begin{cases} \dot{\theta}_{1m} = \dfrac{H_{td}}{I_{con}} - 2(m_1 + m_2)\dfrac{H_{td}}{I_{con}} l_{com}(d - l_0) - \dfrac{J_2}{I_{con}}\dot{\theta}_2 \\ \theta_{1m}(t) = \theta_{10} + \dfrac{H_{td}}{I_{con}} t - 2H_c(m_1 + m_2)\dfrac{l_{com}}{I_{con}^2} \\ \qquad \int_0^t (d - l_0)\,dt - \dfrac{J_2}{I_{con}}(\theta_{2s}(t) - \theta_{2s}(0)) \\ \dot{\theta}_{1grav}(t) = \left(g\left(m_1\left(l_0 + \dfrac{l_1}{2} \right) + m_2(l_0 + l_1) \right) / I_{con} \right) \int_0^t \theta_1 dt \\ \theta_{1grav}(t) = \int_0^t \dot{\theta}_{1grav}\,dt \end{cases}$$

$$\begin{cases} d = -A\sin(\omega t - \phi) + B \\ H_c = (J_1 + J_2 + m_1(d + l_1/2)^2 + m_2(d + l_1)^2)\dot{\theta}_{1m} + J_2\dot{\theta}_2 \\ t_s = \dfrac{\pi}{\omega} + 2\dfrac{\phi}{\omega} \\ \theta_{2s}(t) = C_s\left(1 - \cos(\omega_{2s} t_s)\right) + D_s . \end{cases}$$

3.2.2 Lift-off transition in matrix form

We express lift-off transition in a matrix, mapping before-lift-off states $x_s^+ = [\theta_{1lo}^-, \dot{\theta}_{1lo}^-, \theta_{2lo}^-, \dot{d}_{lo}]$ to after-lift-off states $x_f^- = [\theta_{1lo}^+, \dot{\theta}_{1lo}^+, \theta_{2lo}^+, \dot{x}_{lo}, \dot{y}_{lo}]$.

$$x_f^- = \underset{s->f}{\Gamma} x_s^+$$
$$\underset{s->f}{\Gamma} = \begin{bmatrix} 1 & 0 & 0 & 0 \\ 0 & 1 & 0 & 0 \\ 0 & 0 & 1 & 0 \\ 0 & Tr_{42} & 0 & \sin(\theta_1) \\ 0 & -Tr_{52} & 0 & \cos(\theta_1) \end{bmatrix}, \quad (10)$$
$$Tr_{42} = \left(\frac{m_1}{m_1 + m_2}\left(d + \frac{l_1}{2} \right)\cos(\theta_1) + \frac{m_2}{m_1 + m_2}\left((d + l_1)\cos(\theta_1) \right) \right)$$
$$Tr_{52} = \left(\frac{m_1}{m_1 + m_2}\left(d + \frac{l_1}{2} \right)\sin(\theta_1) + \frac{m_2}{m_1 + m_2}\left((d + l_1)\sin(\theta_1) \right) \right) .$$

3.2.3 Flight phase dynamics mapping

We calculate the dynamic motion of flight phase into a matrix by mapping after-lift-off states $x_f^- = [\theta_{1lo}^+, \dot{\theta}_{1lo}^+, \theta_{2lo}^+, \dot{x}_{lo}, \dot{y}_{lo}]$ to before-touch-down states $x_f^+ = [\theta_{1td}^-, \dot{\theta}_{1td}^-, \theta_{2td}^-, \dot{x}_{td}, \dot{y}_{td}]$.

$$x_f^+ = A_f x_f^- + B_f \Delta\theta_{2f}$$
$$A_f = \begin{bmatrix} 1 & t_f & 0 & 0 & 0 \\ 0 & 1 & 0 & 0 & 0 \\ 0 & 0 & 1 & 0 & 0 \\ 0 & 0 & 0 & 1 & 0 \\ 0 & 0 & 0 & 0 & -1 \end{bmatrix} \quad B_f = \begin{bmatrix} R_{l/u} \\ 0 \\ 1 \\ 0 \\ 0 \end{bmatrix}, \quad (11)$$
$$R_{l/u} = -(J_2) / \left(J_1 + J_2 + \frac{m_1 m_2}{m_1 + m_2}\left(\frac{l_1}{2} \right)^2 \right),$$

where t_f is flight phase duration, which is considered constant under vertical constraints.

3.2.4 Touch-down transition in matrix form

We calculate the touch-down transition into a matrix, mapping before-touch-down states $x_f^+ = [\theta_{1td}^-, \dot{\theta}_{1td}^-, \theta_{2td}^-, \dot{x}_{td}, \dot{y}_{td}]$ to after touch-down states $x_s^- = [\theta_{1td}^+, \dot{\theta}_{1td}^+, \theta_{2td}^+, \dot{d}_{td}]$

$$x_s^- = \underset{f->s}{\Gamma} x_f^+$$

$$\prod_{f->s} = \begin{bmatrix} 1 & 0 & 0 & 0 & 0 \\ 0 & I_f / I_g & 0 & T_{24} & -T_{25} \\ 0 & 0 & 1 & 0 & 0 \\ 0 & 0 & 0 & \sin(\theta_1) & \cos(\theta_1) \end{bmatrix}, \tag{12}$$

$$T_{25} = \left(m_1 \left(l_0 + l_1 / 2 \right) \sin\left(\theta_{1td}^- \right) + m_2 \left(\left(l_0 + l_1 \right) \sin\left(\theta_{1td}^- \right) \right) \right) / I_s$$

$$T_{24} = \left(m_1 \left(l_0 + l_1 / 2 \right) \cos\left(\theta_{1td}^- \right) + m_2 \left(\left(l_0 + l_1 \right) \cos\left(\theta_{1td}^- \right) \right) \right) / I_s$$

$$x_{con} = \left(\frac{m_1}{m_1 + m_2} \left(l_0 + \frac{l_1}{2} \right) \cos(\theta_{1td}^-) + \frac{m_2}{m_1 + m_2} \left((l_0 + l_1) \cos(\theta_{1td}^-) \right) \right)$$

$$y_{con} = \left(\frac{m_1}{m_1 + m_2} \left(l_0 + \frac{l_1}{2} \right) \sin(\theta_{1td}^-) + \frac{m_2}{m_1 + m_2} \left((l_0 + l_1) \sin(\theta_{1td}^-) \right) \right).$$

The inertia is measured at the center of rotation of each flight and stance phase.

$$I_s = m_1 (l_0 + l_1 / 2)^2 + m_2 \left((l_0 + l_1)^2 \right) + J_1 + J_2$$

$$I_f = m_1 (l_0 + l_1 / 2)^2 + m_2 \left((l_0 + l_1)^2 \right) + J_1 + J_2 - (m_1 + m_2) \left({x_{con}}^2 + {y_{con}}^2 \right).$$

3.3 Poincaré map in mapping matrices

The Poincaré map is derived from approximated matrices below.

$$\begin{cases} x_s^+ = A_s x_s^- + B_s \Delta\theta_{2s} & : x_s^- = [\theta_{1td}^+, \dot{\theta}_{1td}^+, \theta_{2td}^+, \dot{d}_{td}], \\ & \quad x_s^+ = [\theta_{1lo}^-, \dot{\theta}_{1lo}^-, \theta_{2lo}^-, \dot{d}_{lo}] \\ x_f^- = \prod_{s->f} x_s^+ & : x_s^+ = [\theta_{1lo}^-, \dot{\theta}_{1lo}^-, \theta_{2lo}^-, \dot{d}_{lo}], \\ & \quad x_f^- = [\theta_{1lo}^+, \dot{\theta}_{1lo}^+, \theta_{2lo}^+, \dot{x}_{lo}, \dot{y}_{lo}] \\ x_f^+ = A_f x_f^- + B_f \Delta\theta_{2f} & : x_f^- = [\theta_{1lo}^+, \dot{\theta}_{1lo}^+, \theta_{2lo}^+, \dot{x}_{lo}, \dot{y}_{lo}], \\ & \quad x_f^+ = [\theta_{1td}^-, \dot{\theta}_{1td}^-, \theta_{2td}^-, \dot{x}_{td}, \dot{y}_{td}] \\ x_s^- = \prod_{f->s} x_f^+ & : x_f^+ = [\theta_{1td}^-, \dot{\theta}_{1td}^-, \theta_{2td}^-, \dot{x}_{td}, \dot{y}_{td}], \\ & \quad x_s^- = [\theta_{1td}^+, \dot{\theta}_{1td}^+, \theta_{2td}^+, \dot{d}_{td}]. \end{cases} \tag{13}$$

When we select the after-lift-off state as Poincaré section, the Poincaré map shows a discrete control system.

$$x_f^- = \prod_{s->f} (A_s \prod_{f->s} (A_f x_f^- + B_f \Delta\theta_{2f}) + B_s \Delta\theta_{2s})$$

$$x_f^- = \prod_{s->f} A_s \prod_{f->s} A_f x_f^- + \prod_{s->f} B_s \Delta\theta_{2s} + \prod_{s->f} A_s \prod_{f->s} B_f \Delta\theta_{2f}$$

$$\overline{A} = \prod_{s->f} A_s \prod_{f->s} A_f, \quad \overline{B}_1 = \prod_{s->f} B_s, \quad \overline{B}_2 = \prod_{s->f} A_s \prod_{f->s} B_f$$

$$x_f^- = \overline{A} x_f^- + \overline{B}_1 \Delta\theta_{2s} + \overline{B}_2 \Delta\theta_{2f}.$$

3.3.1 Poincaré map and convergence

The modelled Poincaré map consists of linear mapping matrices. This causes a problem whether the Poincaré section state x_f^- converges on a fixed point x_{fix} or not. The fixed point equation includes the control gain K_f and K_g that put all eigenvalues of the Poincaré map within a unit circle. We assume that a fixed point is calculated by desired references c_f and c_s.

$$\begin{aligned} x_{fix} &= \prod_{s->f} A_s \prod_{f->s} (A_f x_{fix} + B_f (K_f (x_{fix} + c_f))) \\ &\quad + \prod_{s->f} B_s (K_s (x_{fix\_s} + c_s)) \\ x_{fix\_s} &= \prod_{f->s} (A_f x_{fix} + B_f (K_f (x_{fix} + c_f))) \\ x_{fix} &= \prod_{s->f} (A_s + B_s K_s) \prod_{f->s} (A_f + B_f K_f) x_{fix} \\ &\quad + \prod_{s->f} (A_s + B_s K_s) \prod_{f->s} B_f K_f c_f \\ &\quad + \prod_{s->f} B_s K_s c_s. \end{aligned} \tag{14}$$

Assuming that the fixed point is calculated by iteration, the sectional state x_{fk+1}^- is calculated by former step state.

$$\begin{aligned} x_{fk+1}^- &= \prod_{s->f_k} (A_{sk} + B_{sk} K_{sk}) \prod_{f->s_k} (A_{fk} + B_{fk} K_{fk}) x_{fk}^- \\ &\quad + \prod_{s->f_k} (A_{sk} + B_{sk} K_{sk}) \prod_{f->s_k} B_{fk} K_{fk} c_f \\ &\quad + \prod_{s->f_k} B_{sk} K_{sk} c_s. \end{aligned} \tag{15}$$

Let the matrices be abbreviated to $\overline{A}_k, \overline{B}_{f(k)}, \overline{B}_{s(k)}$

$$\begin{aligned} \overline{A}_k &= \prod_{s->f_k} (A_{sk} + B_{sk} K_{sk}) \prod_{f->s_k} (A_{fk} + B_{fk} K_{fk}) \\ \overline{B}_{f(k)} &= \prod_{s->f_k} (A_{sk} + B_{sk} K_{sk}) \prod_{f->s_k} B_{fk} K_{fk} \\ \overline{B}_{s(k)} &= \prod_{s->f_k} B_{sk} K_{sk} \\ x_{fk}^- &= \overline{A}_{k-1} x_{fk-1}^- + \overline{B}_{f(k-1)} c_f + \overline{B}_{s(k-1)} c_s \\ x_{fk+1}^- &= \overline{A}_k (\overline{A}_{k-1} x_{fk-1}^- + \overline{B}_{f(k-1)} c_f + \overline{B}_{s(k-1)} c_s) + \overline{B}_{f(k)} c_f + \overline{B}_{s(k)} c_s \\ &= \overline{A}_k \overline{A}_{k-1} x_{fk-1}^- + (\overline{A}_k \overline{B}_{f(k-1)} + \overline{B}_{f(k)}) c_f + (\overline{A}_k \overline{B}_{s(k-1)} + \overline{B}_{s(k)}) c_s \\ x_{fk+1}^- &= \overline{A}_k \overline{A}_{k-1} \left(\overline{A}_{k-1} x_{fk-1}^- + \overline{B}_{f(k-1)} c_f + \overline{B}_{s(k-1)} c_s \right) \\ &\quad + \left(\overline{A}_k \overline{B}_{f(k-1)} + \overline{B}_{f(k)} \right) c_f + (\overline{A}_k \overline{B}_{s(k-1)} + \overline{B}_{s(k)}) c_s \\ x_{fk+1}^- &= \overline{A}_k \overline{A}_{k-1} \overline{A}_{k-2} x_{fk-2}^- \\ &\quad + \left(\overline{A}_k \overline{A}_{k-1} \overline{B}_{f(k-2)} + \overline{A}_k \overline{B}_{f(k-1)} + \overline{B}_{f(k)} \right) c_f \\ &\quad + \left(\overline{A}_k \overline{A}_{k-1} \overline{B}_{s(k-2)} + \overline{A}_k \overline{B}_{s(k-1)} + \overline{B}_{s(k)} \right) c_s. \end{aligned} \tag{16}$$

All eigenvalues of $\overline{A}_k$ exist within a unit circle by feedback inputs K_{fk} and K_{gk}. For sufficiently large k, the following equations are valid.

$$\begin{aligned} x_{fk+1}^- &= (\overline{A}_k \overline{A}_{k-1} \cdots \overline{A}_1 \overline{B}_{f(1)} + \cdots + \overline{A}_k \overline{A}_{k-1} \overline{B}_{f(k-2)} + \overline{A}_k \overline{B}_{f(k-1)} + \overline{B}_{f(k)}) c_f \\ &\quad + (\overline{A}_k \overline{A}_{k-1} \cdots \overline{A}_1 \overline{B}_{s(1)} + \cdots + \overline{A}_k \overline{A}_{k-1} \overline{B}_{s(k-2)} + \overline{A}_k \overline{B}_{s(k-1)} + \overline{B}_{f(k)}) c_s \end{aligned} \tag{17}$$

If the system converges on the fixed point, the matrices converge on fixed values.

$$\bar{A}_k \approx \bar{A}_{fix}, \bar{B}_{f(k)} \approx \bar{B}_{f(fix)}, \bar{B}_{s(k)} \approx \bar{B}_{s(fix)}$$

$$x_{fix} = \left(\bar{A}_{fix}^{k}\bar{B}_{f(fix)} + \cdots + \bar{A}_{fix}^{2}\bar{B}_{f(fix)} + \bar{A}_{fix}\bar{B}_{f(fix)} + \bar{B}_{f(fix)}\right)c_f + \left(\bar{A}_{fix}^{k}\bar{B}_{s(fix)} + \cdots + \bar{A}_{fix}^{2}\bar{B}_{s(fix)} + \bar{A}_{fix}\bar{B}_{s(fix)} + \bar{B}_{s(fix)}\right)c_s$$

$$\bar{A}_{fix}x_{fix} = \left(\bar{A}_{fix}^{k+1}\bar{B}_{f(fix)} + \cdots + \bar{A}_{fix}^{2}\bar{B}_{f(fix)} + \bar{A}_{fix}\bar{B}_{f(fix)}\right)c_f + \left(\bar{A}_{fix}^{k+1}\bar{B}_{s(fix)} + \cdots + \bar{A}_{fix}^{2}\bar{B}_{s(fix)} + \bar{A}_{fix}\bar{B}_{s(fix)}\right)c_s = x_{fix} - \bar{B}_{f(fix)}c_f - \bar{B}_{s(fix)}c_s$$

$$\left(I - \bar{A}_{fix}\right)x_{fix} = \bar{B}_{f(fix)}c_f + \bar{B}_{s(fix)}c_s \quad (18)$$

$\bar{A}_{fix}^{k+1} \approx 0$ for k large enough.

$$x_{fix} = \left(I - \bar{A}_{fix}\right)^{-1}(\bar{B}_{f(fix)}c_f + \bar{B}_{s(fix)}c_s).$$

$\bar{A}_k$ and $\bar{B}_k$ exist and $\bar{A}_k$ converges by control inputs. By definition, $\bar{A}_k$ and $\bar{B}_k$ are matrices calculated at the proximate fixed point and are obtained by a recursive calculation.

4. Gait pattern motion planning and feedback

We simplify the hopping system into a discrete control system with two inputs by approximating the dynamics of the system. The inputs of the discrete control system are upper-body angular displacement of stance phase and flight phase. So we can design a gait pattern by deciding feedback gain. François and Samson [14] introduced feedback of the Poincaré map. They adopted simple massless leg and stance phase motion as an inverted pendulum with no input. Raibert used the foot-placement controller as heuristic feedback and stance phase motion as mirror motion [13]. Poularkakis and Grizzle used a Hybrid zero dynamics (HZD) controller. They used the outer-loop controller of HZD as feedback of Poincaré map [31, 33]. They used foot-placement method at flight phase and LQR feedback at stance phase. These studies focused on stability and feasibility, constraining a continuous phase. We have proposed a method to generate a stable pattern by feedback with constrained motions, using both flight and stance phase motion as inputs. We can generate various motion patterns, such as motion primitives and optimal hopping motions.

4.1 Motion planning

Legged locomotion is hybrid dynamic system. We approximate the dynamics in transverse mapping matrices and build linear Poincaré map. The fixed point of the Poincaré map is a fixed point of gait pattern. We can generate stable gait patterns by finding fixed points.

4.1.1 Motion planning of repeating gait

The motion planning of repeating motion is the problem of creating a fixed point. The fixed point is designed by inputs and references.

4.1.1.1 Designed Gaits

We can design motions by giving input gains and references. The designed motion is a part of gait pattern, which can be considered motion primitives. Once the part of the motion is designed, the rest of the motion is calculated by pole-placement of the Poincaré map.

4.1.1.2 LQR control method

The system is approximated as a discrete MISO system with two inputs. The optimal function is calculated by LQR method.

$$x_f^- = \bar{A}x_f^- + \bar{B}_1\Delta\theta_{2s} + \bar{B}_2\Delta\theta_{2f}$$

$$V_t(x_k) = x_k^T Q x_k + \min_{u_1,u_2}\left(u_1^T R_1 u_1 + u_2^T R_2 u_2 + V_{t+1}\left(A_{fix}x_k + B_{1fix}u_1 + B_{2fix}u_2\right)\right).$$

4.1.2 Motion planning of serial gait

Planning a serial motion of the system is finding paired fixed points. We can design serial gait patterns by combining series of motions.

$$\begin{cases} x_{fixa} = \prod_{s->f_a}(A_{sa} + B_{sa}K_{sa})\prod_{f->s_a}(A_{fa} + B_{fa}K_{fa})x_{fixb} + \prod_{s->f_a}(A_{sa} + B_{sa}K_{sa})\prod_{f->s_a}B_{fa}K_{fa}c_{fa} + \prod_{s->f_a}B_{sa}K_{sa}c_{sa} \\ x_{fixb} = \prod_{s->f_b}(A_{sb} + B_{sb}K_{sb})\prod_{f->s_b}(A_{fb} + B_{fb}K_{fb})x_{fixa} + \prod_{s->f_b}(A_{sb} + B_{sb}K_{sb})\prod_{f->s_b}B_{fb}K_{fb}c_{fb} + \prod_{s->f_b}B_{sb}K_{sb}c_{sb}. \end{cases}$$

5. Simulation

We suggest several patterns which are different from each other and Poincaré stable. The patterns are termed stance-phase motion, motion primitives, hold position, mirror-image motion, double angle motion, and upright motion. We use upper-body displacement as designed motions during stance phase. The upper-body motion during stance phase is given in a trajectory constrained in a sinusoidal function, in Eq. (7).

$$\theta_2(t) = C_s\left(1 - \cos\left(\omega_{2s}t\right)\right) + D_s, \quad \theta_2(t_s) = \theta_{2td}^{+} + \Delta\theta_{2s}.$$

The vertical motion of the hopping system is constrained to compensate the energy loss [5] in Eq. (8).

5.1 Simulation of motion primitives

The simulation is performed with MATLAB ODE45 function of full dynamics.

The upper-body motion during stance phase is expressed in feedback gains as below.

Table 1. Mechanical properties of simulation.

l_0	Spring length	0.29 lm
l_1	Leg length	0.424 m
J_1	Leg inertia	0.103 kgm^2
J_2	Torso inertia	0.101 kgm^2
m_1	Leg mass	4.09 kg
m_2	Torso mass	12.3 kg
$\dot{d}_0$	Radial velocity (Touch-down)	1.5 m/s
K	Spring constant	8000 N/m
g	gravity	9.8 m/s^2

Table 2. Calculated matching feedback gain (gait) and fixed point.

	Feedback gain K_f $\Delta\theta_{2f} = K_s \bar{x}_f^-$	Fixed point x_f^- $[\theta_{1lo}^+, \dot{\theta}_{1lo}^+, \theta_{2lo}^+, \dot{x}_{lo}, \dot{y}_{lo}]$
Hold	[4.69,1.00,0.38,1.36]	[0.00, 0.00,0.36, 0.00,1.0]
Mirror	[2.74,0.55,–0.19,1.55]	[0.02,0.20,-0.14,0.15,0.91]
Double	[2.18,0.95,-0.24,0.74]	[0.01,0.13,-0.12,0.10,0.94]
pright	[2.85,0.60,0.0,1.02]	[0.03,0.30,0.0,0.22,0.87]

$$\begin{cases} K_s = [0 \quad 0 \quad 0 \quad 0] & : \textit{hold position} \\ K_s = [0 \quad 0 \quad -2 \quad 0] & : \textit{mirror image motion} \\ K_s = [0 \quad 0 \quad -3 \quad 0] & : \textit{double angle motion} \\ K_s = [0 \quad 0 \quad -1 \quad 0] & : \textit{upright motion} . \end{cases}$$

We make the MISO discrete control problem of the Poincaré map into SISO system by designing the motion of the stance phase. We can calculate upper-body movement during flight phase, which is feedback that stabilizes the system. The simulation was performed with MATLAB, a full dynamics of hopping system. The controller designed upper-body motion and regulated vertical motion, tracking the references $c_f = [0 \quad 0 \quad 0 \quad -0.1]$ $c_s = [0 \quad 0 \quad 0 \quad 0]$. The feedback gain is calculated at the fixed points, which is a linear value.

Here, $\bar{x}_f^- = [\theta_{1lo}^+, \dot{\theta}_{1lo}^+, \theta_{2lo}^+, \dot{x}_{lo}]$ and the vertical velocity is constrained by total energy control. The total energy at the Apex is regulated.

5.1.1 Simulation result from hold position.

Schematics

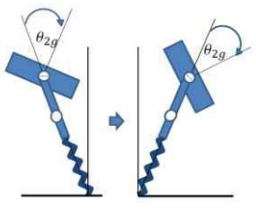

Joint location

$\bar{x} = [x_{joint}, y_{joint}]$

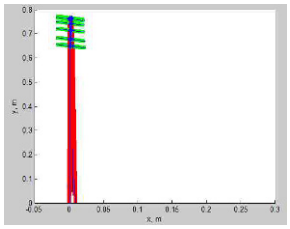

Fixed point

$\bar{x}_f^- = [\theta_{1lo}^+, \theta_{2lo}^+]$

Limit cycle

$\bar{x} = [\theta_1, \theta_2]$

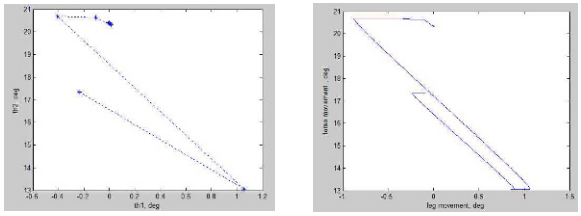

Fig. 4. Simulation of hopping system : Hold position.

The simulation was performed with hold position of the stance phase. The motion is stable and converges to a fixed point, but the total motion of hopper is hopping in one place with inclined upper-body.

5.1.2 Simulation result from mirror-image motion

Schematics

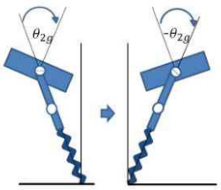

Joint location

$\bar{x} = [x_{joint}, y_{joint}]$

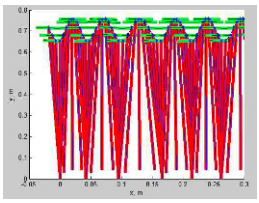

Fixed point

$\bar{x}_f^- = [\theta_{1lo}^+, \theta_{2lo}^+]$

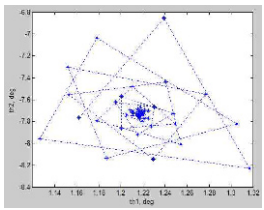

Limit cycle

$\bar{x} = [\theta_1, \theta_2]$

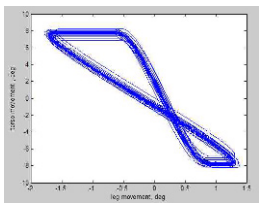

Fig. 5. Simulation of hopping system : Mirror image motion.

The simulation was performed with mirror image motion of stance phase. The system is hopping forwards in a symmetric gait pattern. The motion converges to the fixed point. The input gain is not optimal, as it is calculated at the fixed-point. As a result, the speed of convergence is slow.

5.1.3 Simulation result from double angle motion

Schematics

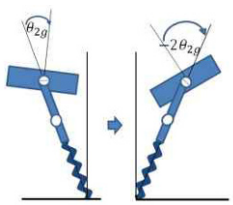

Joint location

$\bar{x} = [x_{joint}, y_{joint}]$

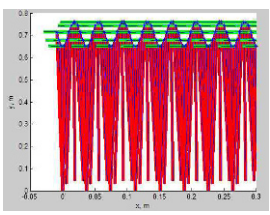

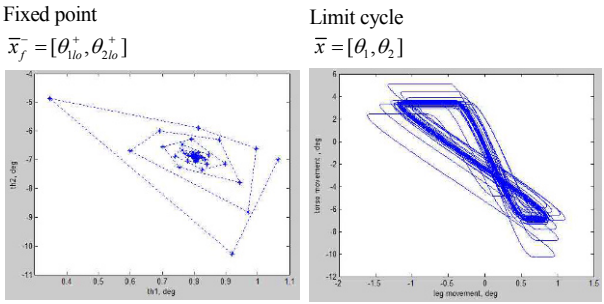

Fig. 6. Simulation of hopping system : Double angle motion.

The simulation is performed with double angle motion of stance phase. The system is hopping forwards in a non-symmetric gait pattern.

5.1.4 Simulation result from upright motion

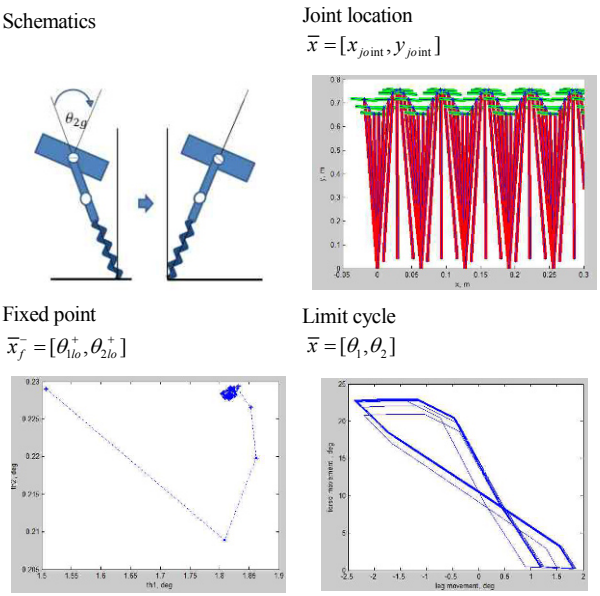

Fig. 7. Simulation of hopping system : Upright motion.

The simulation is performed with upright motion of the stance phase. The system is hopping forwards with a non-symmetric gait pattern. The converging rate of upright motion is fast, as the controller cancels out the initial condition.

5.2 Simulation results

These simulations show that we can generate stable gait patterns by giving stance phase motion and calculating the feedback at flight phase. This includes Raibert's mirror image motion, François and Samson's non-moving stance phase and non-symmetric gaits. We can get a similar result by giving flight phase motion and calculating the feedback at stance phase.

6. Conclusion

We have proposed a method to generate stable gait patterns of a hopping system, using both flight and stance phase upper-body motions. By building a Poincaré map with inputs, we can generate multiple stable motions. We simplify the hopping system to a simple discrete control form. The proposed method involves mapping boundary conditions and inputs. Gait pattern generation is to find a fixed point by combinations of inputs and references. The basic idea of Poincaré map and feedback is a widely accepted control method. However, the linear Poincaré map by approximation of dynamics has narrow range of convergence. As the feedback gain is calculated from modelled linear Poincaré map, the convergence of the system depends on approximation of dynamics and recursive calculation. Therefore, we proposed a method generating stable gait patterns and formulating the hopping system controller by conventional discrete control form, varying by state at fixed points.

Acknowledgment

This work is supported by KAIST, Korea.

Nomenclature

m_1	: Mass of the lower-body
m_2	: Mass of the upper-body
l_1	: Lower body length
j_1	: Inertia of the lower-body
j_2	: Inertia of the upper-body
k	: Spring constant
d	: Spring length
l_0	: Spring length limit
θ_1	: Global angle of the leg (lower-body)
θ_2	: Joint angle of the upper-body
x_s^-	: Boundary condition after touch-down
x_s^+	: Boundary condition before lift-off
x_f^-	: Boundary condition after lift-off
x_f^+	: Boundary condition before touch-down
$\Delta\theta_{2s}$	: Upper-body displacement at stance phase
$\Delta\theta_{2f}$	: Upper-body displacement at flight phase
t_f	: Duration of the flight phase
t_s	: Duration of the stance phase
A_{td}	: Subscript denotes the value of A at touch-down
A_{lo}	: Subscript denotes the value of A at lift-off
A_{com}	: Subscript denotes the value of A of the Center of Mass
A_s	: Subscript denotes the value of A during the stance phase
A_f	: Subscript denotes the value of A during the flight phase
H_{td}	: Angular momentum at touch-down
τ_{grav}	: Torque applied by gravity

References

[1] J. Lygeros et al., *Hybrid systems: modeling, analysis and control* (1999).

[2] M. H. Raibert et al., Experiments in balance with a 3D one-legged hopping machine, *The International J. of Robotics Research,* 3 (1984) 75.

[3] M. H. Raibert, *Dynamically stable legged locomotion*, DTIC Document (1989).

[4] G. Zeglin and B. Brown, *Control of a bow leg hopping robot,* Carriegie Univ. (1998) 793-798.

[5] M. Ahmadi and M. Buehler, Controlled passive dynamic running experiments with the ARL-monopod II, *Robotics, IEEE Transactions on,* 22 (2006) 974-986.

[6] S. H. Hyon and T. Emura, Quasi-periodic gaits of passive one-legged hopper, *Intelligent Robots and Systems 2002, IEEE/RSJ International Conference on* (2002) 2625-2630.

[7] D. E. Koditschek and M. Bühler, Analysis of a simplified hopping robot, *The International J. of Robotics Research,* 10 (1991) 587-605.

[8] W. J. Schwind and D. E. Koditschek, Control of forward velocity for a simplified planar hopping robot, *Robotics and Automation 1995, Proceedings. of 1995 IEEE International Conference on,* 1 (1995) 691-696.

[9] R. Blickhan and R. Full, Similarity in multilegged locomotion: Bouncing like a monopode, *J. of Comparative Physiology A: Neuroethology, Sensory, Neural and Behavioral Physiology,* 173 (1993) 509-517.

[10] I. Poulakakis and J. Grizzle, Monopedal running control: SLIP embedding and virtual constraint controllers, *Intelligent Robots and Systems 2007 (IROS 2007), IEEE/RSJ International Conference on* (2007) 323-330.

[11] I. Poulakakis and J. W. Grizzle, The spring loaded inverted pendulum as the hybrid zero dynamics of an asymmetric hopper, *Automatic Control, IEEE Transactions on,* 54 (2009) 1779-1793.

[12] I. Poulakakis and J. Grizzle, Formal embedding of the spring loaded inverted pendulum in an asymmetric hopper, *Intelligent Robots and Systems 2007 (IROS 2007), IEEE/RSJ International Conference on* (2007).

[13] M. H. Raibert and E. R. Tello, Legged robots that balance, *IEEE Expert,* 1 (1986) 89-89.

[14] C. François and C. Samson, A new approach to the control of the planar one-legged hopper, *The International J. of Robotics Research,* 17 (1998) 1150-1166.

[15] B. Morris and J. Grizzle, A restricted poincaré map for determining exponentially stable periodic orbits in systems with impulse effects: application to bipedal robots, *Decision and Control 2005 and 2005 European Control Conference. CDC-ECC '05. 44th IEEE Conference on* (2005).

[16] J. Morimoto et al., Poincare-map-based reinforcement learning for biped walking, *Robotics and Automation 2005 (ICRA 2005), Proceedings of the 2005 IEEE International Conference on* (2005) 2381-2386.

[17] R. Altendorfer et al., Stability analysis of legged locomotion models by symmetry-factored return maps, *The International J. of Robotics Research,* 23 (2004) 979-999.

[18] M. Y. Cheng and C. S. Lin, Measurement of robustness for biped locomotion using linearized Poincare'map, *Systems, Man and Cybernetics 1995, Intelligent Systems for the 21st Century., IEEE International Conference on,* 2 (1995) 1321-1326.

[19] Y. Sugimoto and K. Osuka, Stability analysis of passive-dynamic-walking focusing on the inner structure of Poincare map, *Advanced Robotics 2005, ICAR '05, Proceedings. of 12th International Conference on* (2005) 236-241.

[20] W. J. Schwind and D. E. Koditschek, Approximating the stance map of a 2-DOF monoped runner, *J. of Nonlinear Science,* 10 (2000) 533-568.

[21] H. Geyer et al., Spring-mass running: simple approximate solution and application to gait stability, *J. of Theoretical Biology,* 232 (2005) 315-328.

[22] U. Saranlı et al., Approximate analytic solutions to non-symmetric stance trajectories of the passive Spring-Loaded Inverted Pendulum with damping, *Nonlinear Dynamics,* 62 (2010) 729-742.

[23] J. Pratt et al., Capturability-based analysis and control of legged locomotion, part 2: Application to m2v2, a lower body humanoid, *The International J. of Robotics Research,* 0278364912452762 (2012).

[24] I. R. Manchester et al., Stable dynamic walking over uneven terrain, *The International J. of Robotics Research,* 0278364910395339 (2011).

[25] J. W. H. Grizzle, B. Morris and H.-W. Park, MABEL a new robotic bipedal walker and runner, *American Control Conference*, *ACC '09* (2009).

[26] A. Sayyad et al., Single-legged hopping robotics research—A review: A review, *Robotica,* 25 (2007) 587-613.

[27] H. Rad et al., Design, modeling and control of a hopping robot, *Intelligent Robots and Systems '93, IROS '93, Proceedings of the 1993 IEEE/RSJ International Conference on* (1993) 1778-1785.

[28] M. Ankarali et al., An analytical solution to the stance dynamics of passive spring-loaded inverted pendulum with damping, *12th International Conference on Climbing and Walking Robots and the Support Technologies for Mobile Machines (CLAWAR'09),* Istanbul, Turkey (2009).

[29] O. Arslan et al., An approximate stance map of the spring mass hopper with gravity correction for nonsymmetric locomotions, *Robotics and Automation 2009, ICRA '09, IEEE International Conference on* (2009) 2388-2393.

[30] P. Holmes, Poincaré, celestial mechanics, dynamical-systems theory and 'chaos', *Physics Reports,* 193 (1990) 137-163.

[31] I. Poulakakis and J. Grizzle, Modeling and control of the monopedal robot thumper, *Robotics and Automation 2009, ICRA '09. IEEE International Conference on* (2009) 3327-3334.

[32] P. Morin and C. Samson, Trajectory tracking for non-holonomic vehicles: overview and case study, *IEEE*

Workshop on Robot Motion Control (RoMoCo) (2004) 139-153.

[33] E. Westervelt et al., Hybrid zero dynamics of planar biped walkers, *Automatic Control, IEEE Transactions on,* 48 (2003) 42-56.

Appendix

Eq. (2) is shown as below:

$$\begin{cases} \left(J_1+J_2+m_1\left(d+\frac{l_1}{2}\right)^2+m_2\left(d+l_1\right)^2\right)\ddot{\theta}_1+J_2\ddot{\theta}_2 \\ \quad +2\left(m_1+m_2\right)d\dot{d}\dot{\theta}_1+\left(m_1+2m_2\right)\dot{d}l_1\dot{\theta}_1 \\ =m_2g\sin\left(\theta_1\right)\left(d+l_1\right)+m_1g\sin\theta_1\left(d+\frac{l_1}{2}\right) \\ J_2\ddot{\theta}_1+J_2\ddot{\theta}_2=\tau_2 \\ \left(m_1+m_2\right)\ddot{d}+K(d-d_0)-\left(m_1+m_2\right)d\dot{\theta}_1^2-\left(\frac{m_1}{2}+m_2\right)l_1\dot{\theta}_1^2 \\ =-\left(m_1+m_2\right)g\cos\left(\theta_1\right)+f\,. \end{cases}$$

The contact point acts as a hinge.

Eq. (3) is shown as below:

$$\begin{cases} \theta_{1lo}^+=\theta_{1lo}^- \\ \dot{\theta}_{1lo}^+=\dot{\theta}_{1lo}^- \\ \theta_{2lo}^+=\theta_{2lo}^- \\ \dot{\theta}_{2lo}^+=\dot{\theta}_{2lo}^- \\ x_{lo}=\frac{m_1}{m_1+m_2}\left(d+\frac{l_1}{2}\right)\sin\left(\theta_{1lo}^-\right)+\frac{m_2}{m_1+m_2}\left(d+l_1\right)\sin\left(\theta_{1lo}^-\right) \\ \dot{x}_{lo}=\left(\frac{m_1}{m_1+m_2}\left(d+\frac{l_1}{2}\right)\cos\left(\theta_{1lo}^-\right)+\frac{m_2}{m_1+m_2}\left(d+l_1\right)\cos\left(\theta_{1lo}^-\right)\right) \\ \quad \dot{\theta}_{1lo}^-+\dot{d}_{lo}\sin\left(\theta_{1lo}^-\right) \\ y_{lo}=\frac{m_1}{m_1+m_2}\left(d+\frac{l_1}{2}\right)\cos\left(\theta_{1lo}^-\right)+\frac{m_2}{m_1+m_2}\left(d+l_1\right)\cos\left(\theta_{1lo}^-\right) \\ \dot{y}_{lo}=-\left(\frac{m_1}{m_1+m_2}\left(d+\frac{l_1}{2}\right)\sin\left(\theta_{1lo}^-\right)+\frac{m_2}{m_1+m_2}\left(d+l_1\right)\sin\left(\theta_{1lo}^-\right)\right) \\ \quad \dot{\theta}_{1lo}^-+\dot{d}_{lo}\cos\left(\theta_{1lo}^-\right)\,. \end{cases}$$

Eq. (4) is shown as below:

$$\begin{cases} J_1+J_2+\frac{m_1m_2}{m_1+m_2}\left(\frac{l_1}{2}\right)^2\ddot{\theta}_1+J_2\ddot{\theta}_2=0 \\ J_2\ddot{\theta}_1+J_2\ddot{\theta}_2=\tau_2 \\ \left(m_1+m_2\right)\ddot{x}=0 \\ \left(m_1+m_2\right)\ddot{y}=-\left(m_1+m_2\right)g\,. \end{cases}$$

Assuming the external torque and force is not applied.

Eq. (5) is shown as below:

$$\begin{cases} \theta_{1td}^+=\theta_{1td}^- \\ \dot{\theta}_{1td}^+=I_f/I_g\dot{\theta}_{1td}^-+f_1\left(\theta_{1td}^-\right)\dot{x}_{td}+f_2\left(\theta_{1td}^-\right)\dot{y}_{td} \\ \theta_{2td}^+=\theta_{2td}^- \\ \dot{\theta}_{2td}^+=\dot{\theta}_{2td}^- \\ d_{td}=l_0 \\ \dot{d}_{td}=\sin\left(\theta_{1td}^-\right)\dot{x}_{td}+\cos\left(\theta_{1td}^-\right)\dot{y}_{td}\,. \end{cases}$$

HyangJun Lee is a Ph.D. candidate in the HUBOLAB, KAIST, Korea, in 2015. His research area is the legged locomotion system.

Jun Ho Oh is a Professor in the HUBOLAB, KAIST, Korea, in 2015. His research area is the legged locomotion system.